Diagn Interv Radiol 2017; 23:187–193

CARDIOVASCULAR IMAGING

REVIEW

Spectral detector CT for cardiovascular applications

Prabhakar Rajiah
Suhny Abbara
Sandra Simon Halliburton

ABSTRACT

Spectral detector computed tomography (SDCT) is a novel technology that uses two layers of detectors to simultaneously collect low and high energy data. Spectral data is used to generate conventional polyenergetic images as well as dedicated spectral images including virtual monoenergetic and material composition (iodine-only, virtual unenhanced, effective atomic number) images. This paper provides an overview of SDCT technology and a description of some spectral image types. The potential utility of SDCT for cardiovascular imaging and the impact of this new technology on radiation and contrast dose are discussed through presentation of initial patient studies performed on a SDCT scanner. The value of SDCT for salvaging suboptimal studies including those with poor contrast-enhancement or beam hardening artifacts through retrospective reconstruction of spectral data is discussed. Additionally, examples of specific benefits for the evaluation of aortic disease, imaging before transcatheter aortic valve implantation, evaluation of pulmonary veins pre- and post-pulmonary radiofrequency ablation, evaluation of coronary artery lumen, assessment of myocardial perfusion, detection of pulmonary embolism, and characterization of incidental findings are presented.

In spectral computed tomography (CT), multiple spectrally distinct attenuation data sets are obtained from the same scan, which enables material composition analysis not possible with conventional CT. Dual-energy CT (DECT), where a low and high energy data set are obtained, is currently available in clinical practice using the following approaches: a) Dual source technology: two x-ray tube/detector systems separated by approximately 90° and operated at different tube potentials (1) (Fig. 1a); b) Rapid tube potential switching technology: the potential applied across a single x-ray tube is switched rapidly between a high and low setting (1, 2) (Fig. 1b); c) Dual-spin technology: the same anatomical region is scanned twice during two consecutive rotations, once with a high potential applied across the x-ray tube and once with a low potential applied (1) (Fig. 1c); d) Split-beam technology: the spectrum emitted from a single tube is split into high and low energy spectra (3).

Spectral detector CT (SDCT) (IQon, Philips Healthcare) is a novel technology introduced for clinical DECT data acquisition. A single potential is applied across a single x-ray tube and two layers of detectors separate low and high energy data: the top layer absorbs low energy photons and the bottom layer absorbs high energy photons (Fig. 1d). In addition to conventional (polyenergetic) images, projection data simultaneously obtained from both detector layers can also be utilized to generate spectral images. The spectral images useful for cardiovascular assessment include virtual monoenergetic images (Fig. 2a), iodine density maps (Fig. 2b), virtual unenhanced images (Fig. 2c), and effective atomic number ($Z_{effective}$) images (Fig. 2d). An important feature of SDCT technology is that spectral information is available in all patients without *a priori* selection of a special protocol or exposure to additional radiation. Images are available at full field-of-view and a minimum rotation time of 0.27 seconds (s) with complete temporal and spatial registration.

In this paper, we present our initial clinical experience based on the acquisition of data from over 200 patients who underwent cardiovascular studies (i.e., cardiac, aorta, pulmonary veins, pulmonary arteries) using SDCT including the impact of this technology on radiation dose and contrast dose. The creation of spectral images from spectral data is discussed and the utility of these images is demonstrated for specific cardiovascular applications.

From the Department of Radiology (P.R. ✉ *radprabhakar@gmail.com*, S.A.) Southwestern Medical Center, Dallas, Texas, USA; Philips Healthcare (S.S.H.) Cleveland, Ohio, USA.

Received 10 May 2016; revision requested 10 July 2016; revision received 26 July 2016; accepted 17 September 2016.

Published online 17 March 2017.
DOI 10.5152/dir.2016.16255

SDCT scanning

The SDCT scanner (IQon, Philips Healthcare) has a single x-ray source operated at a fixed tube potential (80, 100, 120, or 140 kVp) but two layers of detectors: a top layer of low atomic number (Z) yttrium-based garnet detector and a bottom layer of Gadolinium oxysulphide (Fig. 1). These detectors record two distinct energy spectra, with the top layer absorbing low energy photons and the bottom layer absorbing high energy photons. The prototype system used in our institution to gain initial experience has a collimated detector width of 64×0.625 mm, which yields 40 mm z-coverage and a gantry rotation time of 0.27 s. The SDCT system uses the same scanning protocols as those used for a conventional CT scanner (iCT SP, Philips Healthcare). Scans can be performed with prospective or retrospective electrocardiography (ECG) gating. Conventional polyenergetic images (e.g., 120 kVp) are reconstructed for every patient. Iterative reconstruction algorithms can be applied to the conventional images.

Spectral images

Simultaneous acquisition of aligned high and low energy x-ray spectra allows projection-based spectral decomposition of the data into individual basis components with differing energy dependencies, specifically photoelectric effect and Compton scatter components. After decomposition, the data are reconstructed to obtain basis pair images (1, 4). The photoelectric and Compton basis pair images can then be processed to obtain several types of spectral images including both attenuation-based and nonattenuation-based images.

Virtual monoenergetic images

Virtual monoenergetic images which display tissue attenuation properties similar to those resulting from imaging with a monoenergetic beam at a single kiloelectron voltage (keV) level, can be created from a linear combination of photoelectric and Compton images (4). The voxels display attenuation values in Hounsfield Units (HUs) that change with changing keV level. Virtual monoenergetic images can be generated at energy levels ranging from 40 to 200 keV (Fig. 2a). In this scanner, 70 keV images are the monoequivalent of conventional 120 kVp images for adult body scans, meaning that the resulting HU values closely match those from polychromatic images obtained at 120 kVp.

Low energy monoenergetic images are heavily influenced by photoelectric data and useful in boosting vascular contrast. At lower x-ray energies, the attenuation of iodine is higher; CT numbers of iodine are 70% higher in images acquired with a peak tube potential of 80 kVp compared with images acquired at 140 kVp (5). As higher energies are utilized, images become dominated by Compton scatter and are more useful for decreasing artifacts. The polyenergetic nature of the x-ray beam leads to "hardening" of the beam as it passes through the patient: low energy photons are preferentially attenuated such that the beam contains a lower percentage of low energy photons as it exits the patient compared with when it enters the patient. Thus, x-ray projections passing through a highly attenuating tissue or object (e.g., enhanced blood, calcium, metal) yield CT numbers that are artificially lowered adjacent to and radiating from the area of high attenuation. These beam hardening artifacts are minimized on images generated from higher virtual monoenergetic beams (e.g., ≥70 keV) (5), particularly when basis pairs are obtained using projection-based decomposition as is possible with SDCT because of perfect spatial and temporal alignment of the dual energy data sets.

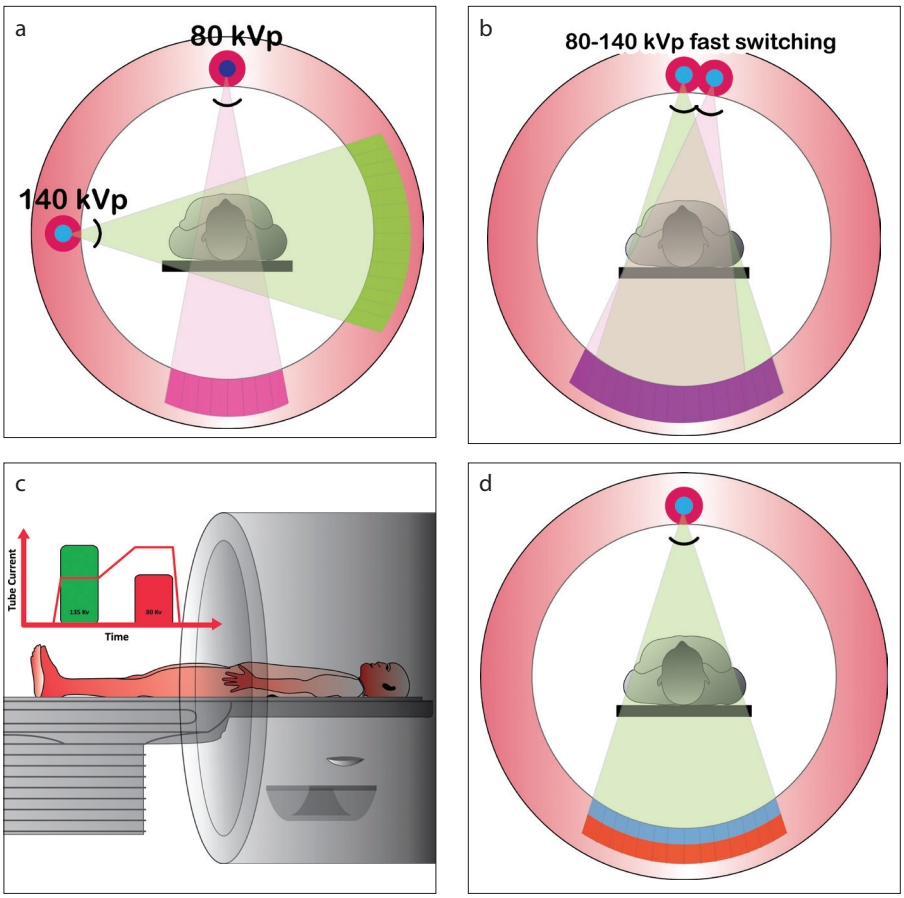

Figure 1. a–d. Illustration showing different types of dual energy CT scanners. Dual source scanner **(a)**: in this type of technology, there are two x-ray sources, which are operated at different energies (for example, 80 and 140 kVp). Rapid kVp switching **(b)**: at each x-ray projection, the kVp is rapidly switched between low (80 kVp) and high energy (140 kVp) levels. Dual spin technology **(c)**: using a volume scanner, the patient is initially scanned at one energy level (135 kVp) and immediately scanned in the same anatomic location using a different energy level (80 kVp). Dual layer or spectral detector CT (SDCT) **(d)**: in this technology, there is one x-ray source, but there are two layers of detectors, with the top layer *(blue)* absorbing low energy photons and the bottom layer *(red)* absorbing high energy photons.

Main points

- Spectral detector CT is a novel technology that uses two layers of detectors to simultaneously collect low and high energy data.
- Virtual monoenergetic images at low energies are useful in improving contrast signal, thus helpful in salvaging suboptimal vascular studies or prospectively use low dose of intravenous contrast.
- Virtual monoenergetic images at high energies are useful in reducing artifacts.
- Spectral detector CT is useful in myocardial perfusion.

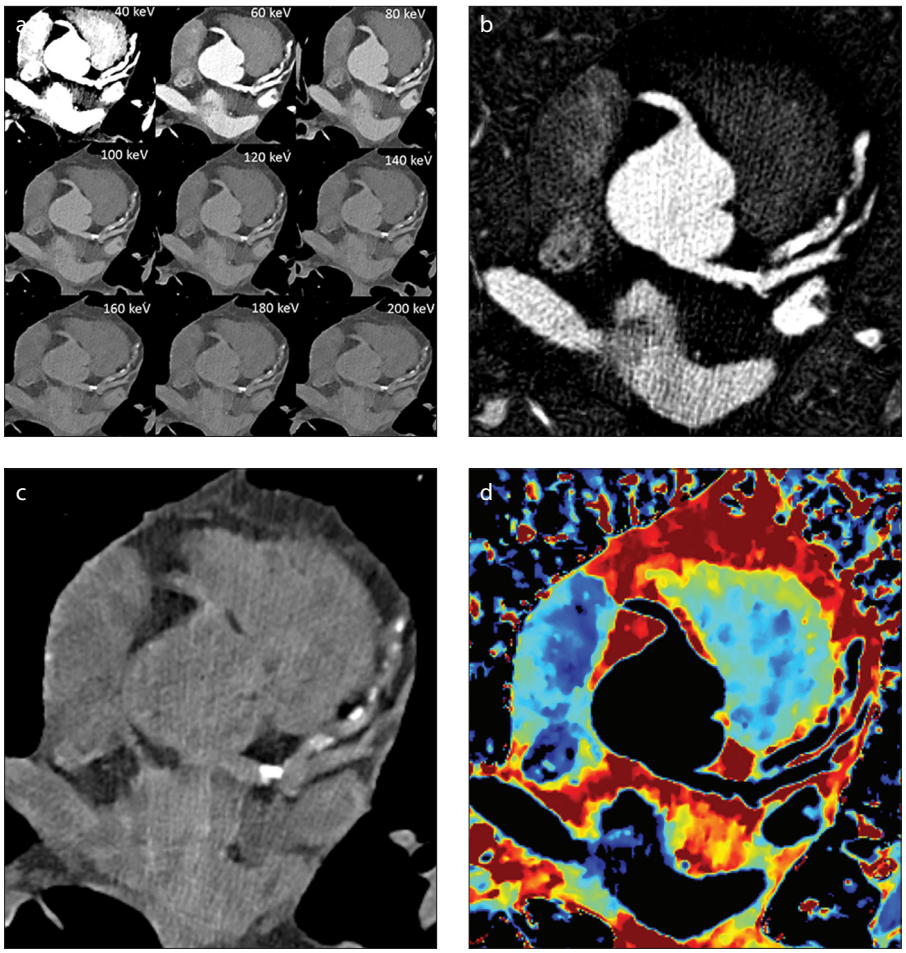

Figure 2. a–d. Types of spectral images. Panel **(a)** shows cross-section of the heart displayed as virtual monoenergetic images from 40 to 200 keV displaying tissue attenuation properties similar to those resulting from imaging with a monoenergetic beam at a single keV level. Panel **(b)** shows iodine density maps in which pixels containing iodine are preserved but all other pixels appear black. Panel **(c)** displays virtual unenhanced images in which pixels containing iodine have been removed. Panel **(d)** shows effective atomic number ($Z_{effective}$) images; pixel values equal $Z_{effective}$ of tissue contained within each voxel.

Iodine density maps

Photoelectric and Compton basis images can also be used to separate (decompose) unknown tissue within a voxel into selected material pairs (e.g., iodine and water) with known attenuation properties at high and low energies. This approach can be used to generate iodine density maps (a.k.a., iodine, no water) (1). In iodine density maps, pixels containing iodine are preserved but all other pixels appear black (Fig. 2b). Iodine, density maps display iodine density in units of mg/mL for quantification of iodine. Iodine maps can either be presented as grayscale images or overlaid as color on attenuation images.

Virtual unenhanced images

Alternatively, tissue decomposition can also be used to remove iodine content from an image (no iodine image) (Fig. 2c). In virtual unenhanced images, iodinated pixels are replaced by virtual attenuation values equivalent to the attenuation of the tissue contained within each pixel in the absence of contrast (1). Pixels not containing iodine retain original attenuation values.

Effective atomic number images

The availability of high and low energy spectra and subsequent decomposition enables characterization of tissues based on effective atomic number ($Z_{effective}$). $Z_{effective}$ is a weighted average of the atomic numbers of elements in a composite substance and is sensitive to the concentration of individual elements. $Z_{effective}$ images or maps, where pixel values equal $Z_{effective}$ of the tissue contained within each voxel (Fig. 2d), may allow discrimination of tissue beyond what is possible with attenuation-based images. $Z_{effective}$ maps can be displayed as grayscale images or overlaid as color on attenuation images (1).

Clinical cardiovascular scenarios

Early clinical experience with SDCT has demonstrated many potential areas for application of this technology to cardiovascular imaging. First we describe two general situations that could arise in any cardiovascular application, poor contrast enhancement and significant beam hardening artifacts, and describe the utility of SDCT for improving diagnostic quality. Then, we present some benefits of SDCT for specific cardiovascular indications.

Poor contrast enhancement

Suboptimal contrast enhancement can occur in routine CT angiographic studies usually due to contrast extravasation, patient factors, or injection-scan timing factors. This can necessitate a repeat study, resulting in additional contrast and radiation dose. Data acquisition with SDCT may obviate the need for a repeat study in these cases because of the availability of spectral data for generation of virtual monoenergetic images at low energies (Fig. 3). Low energy monoenergetic images can elevate iodine attenuation to levels comparable to those on conventional images obtained with higher volumes of contrast (5). It can also be inferred that data from a routine chest or abdomen scan where contrast is optimized for evaluating parenchymal abnormalities can be rendered useful for angiographic assessment of, for example, the pulmonary arteries or aorta, by creating low energy monoenergetic images and boosting vascular contrast. This may be useful for increasing diagnostic confidence of vascular abnormalities, such as pulmonary embolism detected incidentally in a routine CT of the chest.

Beam hardening artifacts

Beam hardening artifacts often arise from areas of high iodine concentration in the subclavian veins or the superior vena cava during cardiovascular CT angiography. Such artifacts are largely mitigated with appropriate contrast injection protocols (e.g., contrast injection followed by saline flush) but, because of the unpredictability of enhancement in a given patient, cannot be completely avoided. The availability of spectral data for all patients regardless of the selected data acquisition protocol permits generation of virtual monoenergetic images if needed. Beam hardening artifacts are minimized on high monoenergetic images (6). Beam hardening artifacts also arise from high attenuating implanted objects such as stents or pacing wires common in cardiovas-

cular patients. Dual energy data has been shown to be effective in decreasing various beam hardening artifacts (6–8). Again, with SDCT, the spectral data necessary to create virtual high monoenergetic images is available by default if incidentally encountered artifacts interfere with image evaluation.

Evaluation of aortic disease

Patients being evaluated for suspected aortic syndrome or followed after endovascular stent graft repair often require multiphase imaging. Virtual unenhanced images can be created from arterial phase or venous phase data acquired with DECT and used in place of true unenhanced images (Fig. 4). This eliminates the need for unenhanced scanning and significantly decreases radiation dose. The utility of virtual unenhanced images for evaluation of the aorta has been demonstrated convincingly with other dual energy technologies (9–11).

Assessment before transcatheter aortic valve implantation (TAVI)

Patients are evaluated with CT prior to transcatheter aortic valve implantation (TAVI) to measure the aortic annulus, aortic root, distance from annulus to coronary ostia, optimal angiographic angle; evaluate the access vessels for size and significant atherosclerosis; and assess the aorta for aneurysm, dissection, and extensive plaque (12). Low contrast dose is preferred in many TAVI patients with severe renal dysfunction, in whom the intravenous administration of iodinated contrast can result in kidney damage (13). With SDCT, a very low volume of contrast can be given for high-risk TAVI patients and virtual low monoenergetic (e.g., 50 keV) images created that boost iodine attenuation to levels comparable to those on conventional images obtained with higher volumes of contrast (Fig. 5) (14). Virtual low energy monoenergetic images have been shown to boost vascular contrast in several vascular beds (15–17). The necessary measurements can be made from the virtual monoenergetic images permitting imaging with equivalent radiation dose but lower contrast dose compared with standard single energy CT.

Pulmonary vein imaging

CT is used in patients being evaluated for pulmonary venous ostial radiofrequency ablation for atrial fibrillation, before the procedure for venous anatomy, ostial sizes, and thrombus and after the procedure for complications. Thrombus in the left atrial appendage (LAA) should be distinguished from slow flow, with the former requiring anticoagulant therapy. Attenuation values can be used to make a diagnosis, with lower attenuation favoring thrombus. A ratio of LAA to ascending aorta (AAo) attenuation greater than 0.75 has 100% negative predictive value (18). Delayed phase images are also helpful, since slow flow disappears during this phase, whereas thrombus persists. The LAA/AAo ratio is lower for thrombus (0.29±12) than slow flow (0.85±12) as measured from delayed phase images (19).

Alternatively with SDCT, the iodine concentration of the region-of-interest can be measured directly from iodine maps generated from spectral data obtained during arterial phase imaging. Thrombus has lower iodine concentration (Fig. 6) than slow flow. Hur et al. (20) have demonstrated that a dual-energy based iodine concentration cutoff threshold of 1.74 mg/mL can distinguish thrombus from slow flow with 100% sensitivity, 100% specificity, and area under the receiver operating characteristics curve of 1.00, when correlated with echocardiography. In this way, SDCT can spare radiation dose and shorten CT examination time, by eliminating the need for an additional delayed imaging phase in these patients.

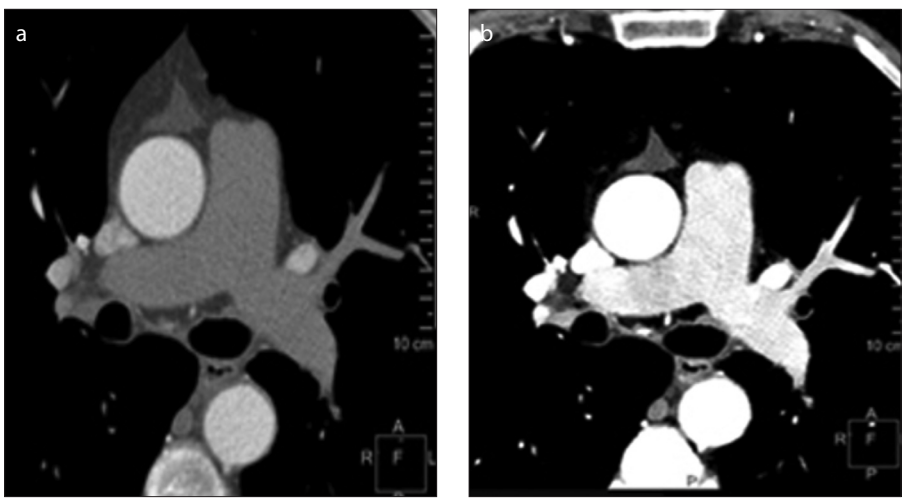

Figure 3. a, b. Salvage of a suboptimal pulmonary embolism study. Conventional polyenergetic CT image **(a)** obtained for evaluation of pulmonary embolism with poor vascular enhancement due to contrast extravasation. Virtual 40 keV monoenergetic image **(b)** shows significantly improved enhancement permitting evaluation of the pulmonary arteries, obviating the need for a repeat contrast injection.

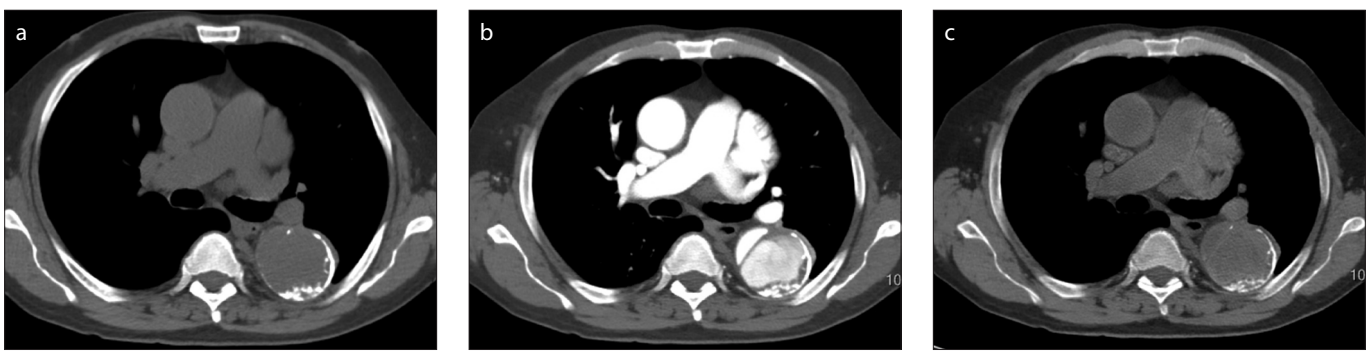

Figure 4. a–c. Equivalency of virtual unenhanced image to true unenhanced image in patient evaluated for acute chest pain. Conventional polyenergetic axial CT image of the chest **(a)** obtained before the injection of contrast showing no contrast in the aorta and other vascular structures. Conventional contrast-enhanced image **(b)** obtained just after contrast injection showing increased attenuation in the aorta. Virtual unenhanced image **(c)** created from spectral data obtained just after contrast injection. Like the true unenhanced image at approximately the same level, the virtual unenhanced image shows no contrast in the aorta and other vascular structures.

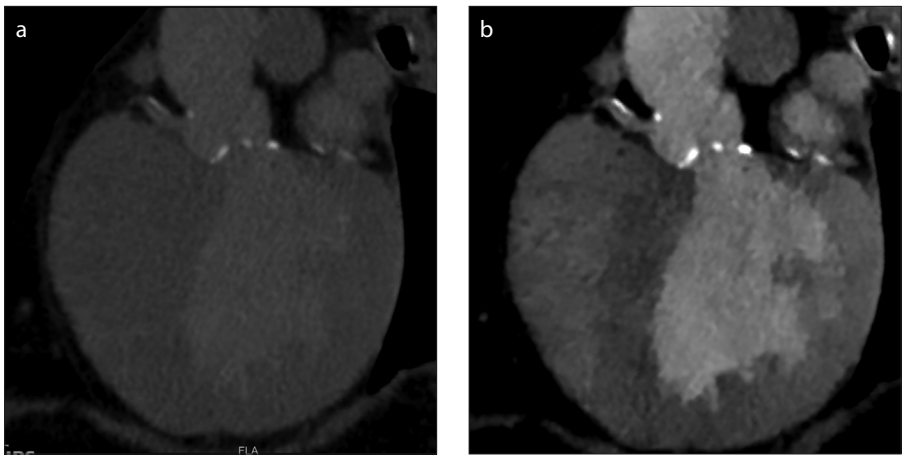

Figure 5. a, b. Administration of low volume of contrast in a patient imaged for evaluation prior to percutaneous aortic valvular implantation. Conventional polyenergetic CT image **(a)** in a patient after injection of 20 mL of iodinated contrast shows suboptimal blood pool enhancement. Virtual 40 keV monoenergetic image **(b)** generated from the same data set at the same level shows significant boosting of contrast within the vessels.

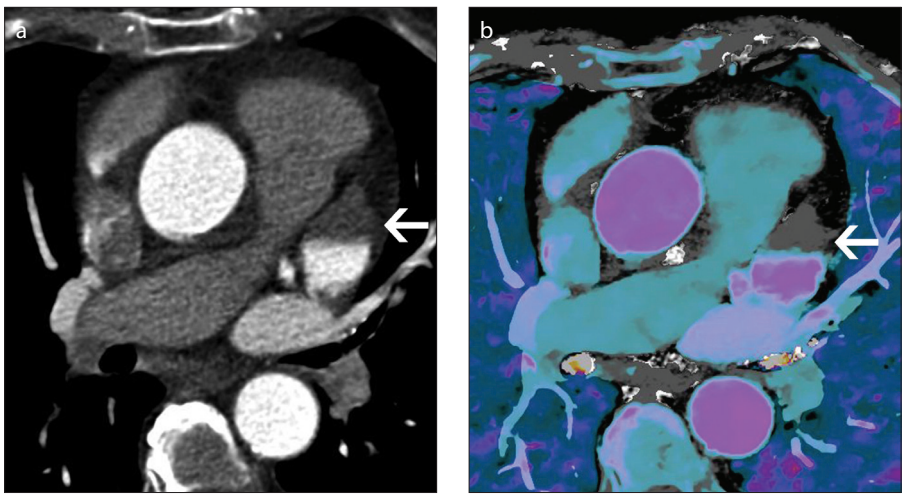

Figure 6. a, b. Distinguishing thrombus and slow flow in a patient referred for pulmonary vein evaluation. Conventional polyenergetic 120 kVp axial CT image **(a)** shows a hypoattenuating lesion in the left atrial appendage *(arrow)* with a mean attenuation of 65 HU which is indeterminate for discriminating thrombus from slow flow. Iodine overlay at the same level shows no significant iodine (0.5 mg/mL) in the lesion *(arrow)* indicating lesion is a thrombus **(b)**.

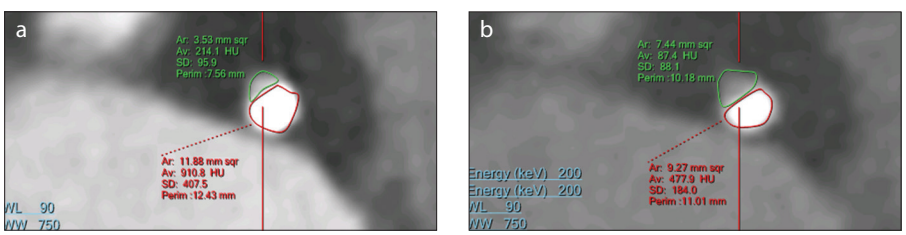

Figure 7. a, b. Reduction in calcium blooming artifact in a patient imaged for atypical chest pain. Conventional polyenergetic CT image **(a)** shows significant calcium blooming in coronary artery, with luminal area of 3.5 mm^2. Panel **(b)** shows 160 keV image with reduced blooming and better defined lumen with area of 7.4 mm^2.

Evaluation of coronary artery lumen

As with other dual energy CT technologies, SDCT may have some utility for the evaluation of coronary artery disease. CT angiography is routinely used for the evaluation of coronary artery stenosis but the calcium extent is often exaggerated (also known as, calcium blooming) causing overestimation of luminal stenosis (21) (Fig. 7a). High monoenergetic images created using projection-based material decomposition were observed to decrease this artifact (22, 23) (Fig. 7b). Clinical studies demonstrating the impact of coronary artery evaluation from high monoenergetic images on the accuracy of stenosis quantification are needed. Additional value for stenosis quantification from high monoenergetic images may also be realized in the presence of stents because of reduced metal artifact.

Myocardial perfusion

CT myocardial perfusion enables evaluation of hemodynamically significant coronary ischemia. CT attenuation can be used to identify myocardial perfusion defects. However, discrimination is often limited by beam hardening artifacts, which mimic lower attenuating, nonviable tissue. Overlay of an iodine map or $Z_{effective}$ map onto attenuation images increases the sensitivity for detection of iodine distribution defects, including ischemia (24, 25). The projection-based material decomposition employed to create these spectral results decreases beam hardening artifacts. Thus, SDCT imaging is thought to make perfusion defects more conspicuous, while also minimizing confounding artifacts (26). Clinical studies are needed to establish if this translates to fewer false positive results with myocardial perfusion CT.

Pulmonary embolism

In acute pulmonary embolism, spectral CT data provide not only direct visualization of an embolus, but also functional information about perfusion, which has prognostic significance (27). Perfusion defects are well-visualized on iodine or $Z_{effective}$ maps. SDCT may be particularly useful in patients with small pulmonary emboli, which may be difficult to visualize on an attenuation-based CT angiogram, but may display a perfusion defect on an iodine or $Z_{effective}$ map, thus improving the sensitivity of detection of these emboli. Chronic pulmonary embolism is visible as a filling defect, which is eccentric or web or band-like and associated with tapering of a vessel. Occasionally, filling defects are not seen or difficult to visualize (Fig. 8a) on a CT angiogram but the patient presents with dyspnea or chronic pulmonary hypertension. Dual energy findings of chronic pulmonary embolism include a mosaic pattern of perfusion defects (Fig. 8b), matched blood pool defects corresponding to occluded arteries, mismatched defects (maintained flow in spite of occlusion due to collaterals) and normal perfusion with normal flow (27). Dual energy CT with existing technologies has already proven useful in the setting of chronic pulmonary embolism because of the ability to obtain anatomical and functional information simultaneously

(27). The SDCT approach may prove additionally useful because of the opportunity to obtain functional data retrospectively if anatomical results alone are inconclusive.

Incidental lesion characterization

Occasionally incidental lesions are seen in cardiovascular images, which typically require further evaluation with additional CT imaging or other imaging studies such as ultrasonography or MRI. The availability of spectral data with every scan performed on the SDCT scanner presents a unique opportunity to help characterize some lesions without the need for additional CT or other imaging studies, potentially reducing additional patient radiation exposure, time to diagnosis and anxiety. Examples include incidental detection of an adrenal lesion. Such a lesion can be characterized using virtual unenhanced images: if the attenuation of the lesion is significantly low, a diagnosis of lipid-rich adenoma can be made without the need for additional imaging (28, 29). Similarly, complex lesions in kidneys, which have high attenuation on conventional arterial phase images, can be further evaluated by using virtual unenhanced images and iodine map (30). These lesions can either be a solid lesion or a complex hemorrhagic cyst. A complicated cyst has high attenuation in the virtual unenhanced image and no iodine in iodine maps, whereas a solid lesion will have low attenuation in virtual unenhanced image but there is significant iodine in iodine maps. Complicated cysts can be followed by imaging, while solid lesions will require biopsy and surgery.

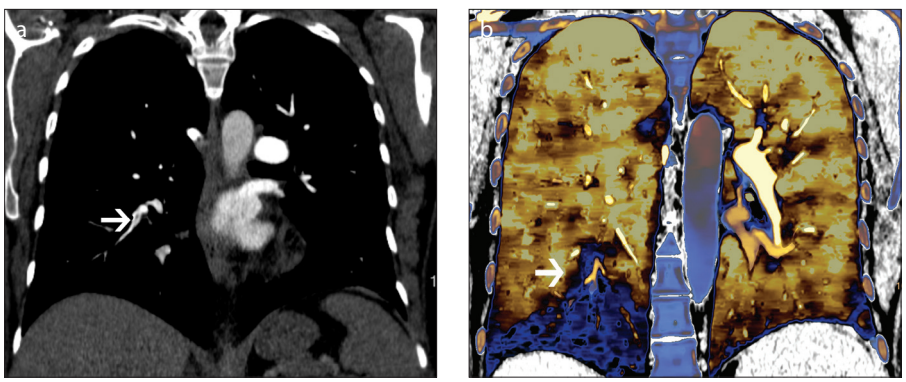

Figure 8. a, b. Perfusion defect from pulmonary embolism. CT pulmonary angiogram **(a)** shows a subtle filling defect in a segmental branch of right lower lobe *(arrow)*. Effective atomic number overlay on conventional image **(b)** shows a peripheral wedge shaped perfusion defect in the right lower lobe *(arrow)*, a consequence of a subtle chronic pulmonary embolism.

Impact on contrast dose and radiation dose

No significant increase in radiation dose has been shown with dual source dual energy technology, while data on rapid kVp switching is inconclusive (31). With SDCT, standard dose saving features for cardiovascular imaging, namely prospective ECG-triggered axial techniques and ECG-based tube current modulation as well as anatomic-based tube current modulation, are utilized. However, spectral separation with SDCT has a minimum tube potential setting of 120 kVp. In order to maintain dose neutrality compared with imaging at a lower tube potential (e.g., 100 kVp) with a standard detector, the tube current must be reduced. In our institution, the protocols on SDCT were ensured to have the same volume CT dose index ($CTDI_{vol}$) as a comparable conventional CT scanner (Philips ICT SP scanner). Opportunities exist for lowering radiation dose with spectral detectors compared with standard detectors primarily through eliminating one phase of a multiphase study, salvaging a suboptimal study that might otherwise need repeating, or obviating the need for follow-up imaging. As with other DECT technologies, the opportunity exists for reducing contrast load with SDCT and exploiting the higher attenuation of iodine at lower energies (5, 14–17). This has

Table. Cardiovascular applications of spectral CT

Application	Clinical uses	Type of spectral image used
Poor contrast enhancement	Boosting vascular attenuation in suboptimally enhanced studies	Virtual monoenergetic image- low energy
	Generating CTA quality images from routine contrast CT (5)	
Beam hardening artifacts	Reduce beam hardening artifacts from dense contrast in veins	Virtual monoenergetic image- high energy
	Reduce artifacts from metal (6–8)	
Evaluation of aortic disease	Radiation dose reduction by eliminating true unenhanced scans by using virtual unenhanced images (9–11)	Virtual unenhanced
Pre-TAVI	Low contrast dose in patients with renal dysfunction (14–17)	Virtual monoenergetic image- low energy
Pulmonary vein imaging	Distinguish left atrial appendage thrombus and slow flow (20)	Iodine map
Evaluation of coronary artery lumen	Decrease calcium blooming and improve lumen definition (22, 23)	Virtual monoenergetic image- high energy
Myocardial perfusion	Improved detection of perfusion defects	Iodine map
	Decreased beam hardening artifacts (24–26)	Virtual monoenergetic image- high energy
Pulmonary embolism	Acute: Improved sensitivity of detection, especially for small defects	Iodine map
	Chronic: Perfusion abnormalities even in the absence of an obvious clot (27)	Effective atomic number map
Incidental lesion characterization	Characterization of incidental nodules, and masses, particularly in kidneys, adrenals and lungs (28)	Virtual unenhanced, iodine map

CT, computed tomography; CTA, CT angiography; TAVI, transcatheter aortic valve implantation.

been demonstrated in special patient populations (e.g., TAVI patients) (14) where there is high motivation to reduce contrast but there is limited experience for imaging of the non-renal-compromised cardiovascular patient.

Comparison of different technologies

With dual-source technology, the kVp and mAs of the tubes can be adjusted independently, with dose optimization for each tube. However, the patients have to be prospectively selected. The projections are asynchronous by 90°. There is smaller field of view (FOV) in one tube and there is also cross scatter. Rapid kVp switching achieves near-synchronous acquisition, enabling projection space decomposition. This technology also requires prospective selection of patients. The mAs cannot be modulated with each kVp switch resulting in variable noise and dose. The gantry rotation time has to be slowed for cardiac scans. Dual spin technology enables optimized mAs and filters for each acquisition, but also requires prospective patient selection. The delay between two acquisitions results in motion and different phases of contrast enhancement (1). Advantages of the SDCT include the ability to retrospectively generate spectral images in all patients without the need to select patient ahead of time. Complete spatial and temporal alignment is not only useful for rapidly moving structures such as the heart, but also enables projection space material decomposition, which is associated with less severe artifacts. There are no FOV, cross-scatter or gantry rotation time limitations. A limitation of this technology is the z-coverage of 4 cm. The cardiovascular applications of SDCT are summarized in the Table.

Conclusion

SDCT is a novel entrant into the field of dual energy CT and has several applications in cardiovascular imaging. The main benefit of this technology stems from the availability of spectral data for every scan, without the need to prospectively select a special acquisition protocol. Virtual monoenergetic images are useful for boosting contrast and reducing artifacts in suboptimal studies. The boosting of iodine attenuation with low energy virtual monoenergetic images also offers the opportunity to reduce the contrast load in renal-compromised patients, including many TAVI patients. The reduction of beam hardening artifacts also has the potential to improve the accuracy of the extent of calcium and the quantification of coronary stenosis. Virtual unenhanced images and iodine maps provide added value from a single data set for distinguishing thrombus from slow flow, identifying areas of myocardial perfusion defect and pulmonary perfusion defect, and characterizing incidental lesions. Virtual unenhanced images may also eliminate the need for acquisition of true unenhanced images in the follow-up of patients with endovascular stents. Although clinical studies are still required to establish the utility of SDCT for specific cardiovascular indications, initial findings are promising.

Conflict of interest disclosure

Prabhakar Rajiah has received institutional research support and honoraria from Philips Healthcare. Suhny Abbara has received institutional research support from Philips Healthcare. Sandra Halliburton is a Philips Healthcare employee.

References

1. Johnson TRC. Dual-energy CT: General principles. Am J Roentgenol 2012; 199: S3–8. [CrossRef]
2. Goodsitt MM, Christodoulou EG, Larson SC. Accuracies of the synthesized monochromatic CT numbers and effective atomic numbers obtained with a rapid kVp switching dual energy CT scanner. Med Phys 2011; 38:2222–2232. [CrossRef]
3. Yu L, Leng S, McCollough CH. Dual-source multi-energy CT with triple or quadruple X-ray beams. Proc SPIE Int Soc Opt Eng 2016; 9783:978312.
4. Alvarez RE, Macovski A. Energy-selective reconstructions in X-ray computerized tomography. Phys Med Biol 1976; 21:633–644. [CrossRef]
5. Vlahos I, Chung R, Nair A, Morgan R. Dual-energy CT: vascular applications. Am J Roentgenol 2012; 199:S87–97. [CrossRef]
6. Yu L, Leng S, McCollough CH. Dual-energy CT-based monochromatic imaging. Am J Roentgenol 2012; 199:S9–15. [CrossRef]
7. Pessis E, Campagna R, Sverzut JM, et al. Virtual monochromatic spectral imaging with fast kilovoltage switching: reduction of metal artifacts at CT. Radiographics 2013; 33:573–583. [CrossRef]
8. Kuchembecker S, Faby S, Sawall S, et al. Dual energy CT: how well can pseudo monochromatic imaging reduce metal artifacts? Med Phys 2015; 42:1023–1036. [CrossRef]
9. Stolzmann P, Frauenfelder T, Pfammatter T, et al. Endoleaks after endovascular abdominal aortic aneurysm repair: detection with dual-energy dual-source CT. Radiology 2008; 249: 682–691. [CrossRef]
10. Numburi UD, Schoenhagen P, Flamm SD, et al. Feasibility of dual-energy CT in the arterial phase: Imaging after endovascular aortic repair. Am J Roentgenol 2010; 195: 486–493. [CrossRef]
11. Sommer WH, Graser A, Becker CR, et al. Image quality of virtual non contrast derived images derived form dual energy CT angiography after endovascular aneurysm repair. J Vasc Interv Radiol 2010; 21:315–321. [CrossRef]
12. Achenbach S, Delgao V, Hausleiter J, et al. SCCT expert consensus document on computed tomography imaging before transcatheter aortic valve implantation (TAVI) transcatheter aortic valve replacement (TAVR). J Cardiovasc Comput Tomogr 2012; 6: 366–380. [CrossRef]
13. Joshi SB, Mendoza DD, Steinberg DH, et al. Ultra-low-dose intra-arterial contrast injection for iliofemoral computed tomographic angiography. JACC Cardiovasc Imaging 2009; 2:1404–1411. [CrossRef]
14. Dubourg B, Caudron J, Lestrat JP, et al. Single-source dual-energy CT angiography with reduced iodine load in patients referred for aortoiliofemoral evaluation before transcatheter aortic valve implantation: impact on image quality and radiation dose. Eur Radiol 2014; 24: 2659–2668. [CrossRef]
15. Nijhof WH, Baltussen EJ, Kant IM, et al. Low-dose CT angiography of abdominal aorta and reduced contrast medium volume: Assessment of image quality and radiation dose. Clinic Radiol 2016; 71:64–73. [CrossRef]
16. Godoy MC, Heller SL, Naidich DP, et al. Dual-energy MDCT: comparison of pulmonary artery enhancement on dedicated CT pulmonary angiography, routine, and low contrast volume studies. Eur J Radiol 2011; 79:e11–17. [CrossRef]
17. Carrascosa P, Leipsic JA, Capunay C, et al. Monochromatic image reconstruction by dual energy imaging allows half iodine load computed tomography coronary angiography. Eur J Radiol 2015; 84:1915–1920. [CrossRef]
18. Patel A, Au E, Donergan K, et al. Multidetector row computed tomography for identification of left atrial appendage filling defects in patients undergoing pulmonary vein isolation for treatment of atrial fibrillation: comparison with transesophageal echocardiography. Heart Rhythm 2008; 5:253–260. [CrossRef]
19. Hur J, Kim JY, Lee HJ, et al. Left atrial appendage thrombi in stroke patients: detection with two-phase cardiac CT angiography versus transesophageal echocardiography. Radiology 2009; 251:683–690. [CrossRef]
20. Hur J, Kim YJ, Lee HJ, et al. Cardioembolic stroke: Dual energy cardiac CT for differentiation for left atrial appendage thrombus and circulatory stasis. Radiology 2012; 263:688–695. [CrossRef]
21. Do S, Karl WC, Liang Z, et al. A decomposition-based CT reconstruction formulation for reducing blooming artifacts. Phys Med Biol 2011; 56:7109–7125. [CrossRef]
22. Boll DT, Merkle EM, Paulson EK, et al. Coronary stent patency: dual- energy multidetector CT assessment in a pilot study with anthropomorphic phantom. Radiology 2008; 247:687–695. [CrossRef]
23. Boll DT, Merkle EM, Paulson EK, et al. Calcified vascular plaque specimens: assessment with cardiac dual energy multidetector CT in anthropomorphically moving heart phantom. Radiology 2008; 249:119–126. [CrossRef]
24. Kang DK, Schoepf UJ, Bastarrika G, et al. Dual-energy computed tomography for integrative imaging of coronary artery disease: principles and clinical applications. Semin Ultrasound CT MR 2010; 31:276–291. [CrossRef]
25. Arnoldi E, Lee YS, Ruzsics B, et al. CT detection of myocardial blood volume deficits: dual-energy CT compared with single-energy CT spectra. J Cardiovasc Comput Tomogr 2011; 5:421–429. [CrossRef]
26. Fahmi R, Eck BL, Levi J, et al. Quantitative myocardial perfusion imaging in porcine ischemia model using a prototype spectral detector CT system. Phys Med Biol 2016; 61:2407–2431. [CrossRef]
27. Lu GM, Zhao YE, Zhang LJ, Schoepf JU. Dual Energy CT of the lung. AJR Am J Roentgenol 2012; 199:540–553. [CrossRef]
28. Mileto A, Nelson RC, Marin D, Roy Choudhury K, Ho LM. Dual-energy multidetector CT for the characterization of incidental adrenal nodules: diagnostic performance of contrast-enhanced material density analysis. Radiology 2015; 274:445–454. [CrossRef]
29. Helck A, Hummel N, Meinel FG, Johnson T, Nikolaou K, Graser A. Can single-phase dual-energy CT reliably identify adrenal adenomas? Eur Radiol 2014; 24:1636–1642. [CrossRef]
30. Graser A, Becker CT, Staehler M, et al. Single-phase dual-energy CT allows for characterization of renal masses as benign or malignant. Invest Radiol 2010; 45:399–405. [CrossRef]
31. Henzler T, Fink C, Schoenberg SO. Dual-energy CT: Radiation dose aspects. AJR Am J Roentgenol 2012; 199:S16–S25. [CrossRef]